IEEE Access
Multidisciplinary | Rapid Review | Open Access Journal

Received 25 July 2022, accepted 3 August 2022, date of publication 8 August 2022, date of current version 11 August 2022.

Digital Object Identifier 10.1109/ACCESS.2022.3197154

RESEARCH ARTICLE

Two-Stage Scheduling Strategy for Integrated Energy Systems Considering Renewable Energy Consumption

XINGHUA LIU[1], (Senior Member, IEEE), SHENGHAN XIE[1], (Student Member, IEEE), JIAQIANG TIAN[1], AND PENG WANG[2], (Fellow, IEEE)

[1]School of Electrical Engineering, Xi'an University of Technology, Xi'an 710048, China
[2]School of Electrical and Electronic Engineering, Nanyang Technological University, Singapore 639798

Corresponding author: Jiaqiang Tian (tianjiaqiang@xaut.edu.cn)

This work was supported in part by the National Natural Science Foundation of China under Grant U2003110, in part by the Key Laboratory Project of Shaanxi Provincial Department of Education under Grant 20JS110.

ABSTRACT With the crisis of energy and environment, the integrated energy systems (IES) have a bright prospect in future energy reform owing to the excellent economic and environmental performance. The IES combines a large amount of renewable energy (RE), which guarantees its economic and environmental benefits. Many uncertainties of RE threaten the performance of IES. How to promote RE consumption under strong uncertainties is a crucial problem in the scheduling of IES. In this work, a two-stage scheduling strategy for IES combining day-ahead scheduling and real-time scheduling is proposed to guide the system operation. The stage of day-ahead scheduling can obtain the optimal scheduling scheme one day in advance based on the forecast data of RE, and the stage of real-time scheduling is introduced to cope with the uncertainties of RE. The model of IES is established based on the energy hub (EH), and the entire strategy is implemented on this model. The model integrates various energy conversion equipment to give full play to the advantages of coordination and complementation of IES. The improved particle swarm optimization (IPSO) is proposed as the solution algorithm of the whole strategy, which improves the traditional PSO through random nonlinearity change inertia weight strategy and best solution perturbation operator (BSPO). Compared with the traditional PSO, IPSO has more excellent performance for solving IES scheduling model. Finally, different schemes under different situations are compared.

INDEX TERMS Integrated energy systems, renewable energy consumption, scheduling strategy, optimal scheduling, particle swarm optimization.

I. INTRODUCTION

The gradual scarcity of fossil energy reserves and the increasingly severe environmental pollution have forced people to reform the existing energy consumption patterns, and IES is an essential technical support for this reform [1], [2], [3], [4], and [5]. Many existing studies have achieved many excellent results in energy trading [6], system modeling [7], and technology integration [8] of IES. However, there are still many challenges in the development process of IES.

In order to achieve the aim of energy conservation and emission reduction, a large amount of RE has been incorporated into IES [9]. The large-scale incorporation of RE is beneficial to the development of IES, and IES is also characterized by its ability to integrate a large amount of RE [10]. However, RE is full of uncertainties in the process of generating power, making it difficult for IES to fully use RE [11]. Therefore, as the amount of RE incorporated into the IES increases, more abandoned energy (AE) appears during the operation of IES, which is a severe waste of RE [12]. If AE can be fully consumed, the economic and environmental benefits of IES must be significantly improved.

The associate editor coordinating the review of this manuscript and approving it for publication was Kuo-Ching Ying.

Therefore, effectively improving RE consumption is a crucial and challenging problem. In recent years, scholars have proposed many methods to improve energy efficiency and RE consumption, which can be roughly divided into energy conversion methods, optimization model methods, forecasting methods, and scheduling strategy.

The energy conversion methods are represented by the power to heat, power to hydrogen, and power to gas (P2G). Literatures [13], [14] investigate the scheduling scheme that transfers abandoned wind and solar energy to electric boilers for heating. However, using electric-thermal coupling equipment to dissipate energy will be restricted by seasons and regions, which makes these schemes don't have universal applicability. Hydrogen conversion technology is employed to convert redundant wind and solar power in [15]. However, this technology is still immature and cannot be used on a large scale in the short term. Advanced technology named P2G is used in [16], [17]. If the energy provided by RE in the system exceeds expectations, the redundant part can be converted into gas through two steps: water electrolysis and methanation. However, the cost of energy conversion equipment applied in P2G is relatively high, which increases the construction cost of the system while increasing RE consumption. On the other hand, P2G technology requires the construction of a large number of gas storage devices, which makes this technology unsuitable for small energy systems.

Methods of optimization model can also improve RE consumption. Literature [18] uses robust optimization to obtain a day-ahead scheduling scheme, which is always robust under the uncertainties of wind and solar power and considers system safety. However, schemes gained by robust optimization are too conservative to schedule, and some economic benefits may be sacrificed. In literature [19], the novel data-driven uncertainty set is employed in the novel two-stage robust optimization model to solve the dispatch problem of multiple microgrids. However, an effective method to overcome the uncertainties of RE has not been proposed, and the phenomenon of energy abandonment caused by uncertainty still exists.

Improving the accuracy of forecast data can also reduce the uncertainties of RE. In literature [20], a weather-based hybrid method for day-ahead hourly forecasting for photovoltaic (PV) units is presented. In [21], a forecasting method for the output power of wind turbines (WTs) and PV units is proposed, which can achieve good prediction accuracy in different weather conditions. Although the forecast accuracy has significantly improved, there is still a gap between the forecast and the actual operation. Therefore, the phenomenon of energy abandonment cannot be wholly avoided.

The methods of scheduling strategy can improve RE consumption by guiding the operation of IES. Scheduling strategies can be divided into three categories according to the time scale: day-ahead scheduling, intra-day scheduling, and real-time scheduling. The above three types of scheduling strategies can be implemented individually or in combination. Literatures [22], [23] implement day-ahead scheduling alone, which can achieve optimal results based on the forecast data of RE, but does not fully consider the uncertainties of RE. In literature [24], day-ahead and intra-day scheduling are combined to reduce the quantity of AE. However, the short-term forecast data used in intra-day scheduling still deviates from the actual operation scenario. Literature [25] combines scheduling strategies of all three time scales and achieves good results, but the process is complicated and requires many computing resources.

Considering preview problems, a two-stage scheduling strategy that can effectively improve energy efficiency and RE consumption of IES under the uncertainties is proposed. The strategy we proposed focuses on the RE consumption rate (RECR) in IES. Through this strategy, the RECR is increased, and the amount of AE is reduced, which can significantly improve the economic and environmental benefits of IES. The original contribution of this work, which differs from the existing studies, can be summarized as follows.

1) The two-stage scheduling strategy can effectively improve energy efficiency and RE consumption by implementing the real-time scheduling stage. This scheduling strategy avoids the high cost and immature energy conversion technologies and is suitable for all levels of IES. The scheduling scheme output by the two-stage scheduling strategy is closer to the requirements of the objective function, and the scheme will not be too conservative.
2) Day-ahead scheduling is combined with real-time scheduling. The scheme obtained from day-ahead scheduling can guide the scheduling work one day in advance, and the scheme obtained in the real-time scheduling stage is used for adjustment based on the day-ahead scheduling scheme. This process fully considers the uncertainties of RE, which are not bound by the accuracy of forecast data. The whole strategy process is concise, which will not occupy too many computing resources.
3) The IPSO is proposed to solve IES scheduling model. A random nonlinear strategy is introduced to change the inertia weight. The BSPO is added to the iterative formula, which can ensure that the solution will not fall into local optimal under the condition of many system balance equation constraints. Through improvement, the probability of falling into a local optimum of IPSO is lower than that of PSO, so the solution accuracy of IPSO is higher. Moreover, the improvement has not destroyed the original advantages of PSO.

The structure of the rest of this paper is organized as follows: Section II designs an IES frame and establishes an IES model based on EH model theory. In Section III, the two-stage scheduling strategy for IES that combines day-ahead scheduling and real-time scheduling is proposed, which can cope with the uncertainties of RE. Section IV validates the superiority of this scheduling strategy through cases study. Finally, the conclusion is summarized in Section V.

II. SYSTEM MODEL

The EH model is used to build the IES model, which can illustrate the conversion and distribution of multiple energy sources [26], [27]. The EH model consumes energy at its entrance, such as power and natural gas infrastructure, and provides necessary energy services at its output side. For the EH model, energy is converted in different forms through coupling devices, including combined heat and power (CHP) units, electric boilers (EB), and absorption chillers [28], [29], [30], and [31].

A variety of energy coupling devices are selected in the IES model of this paper. The schematic diagram of the IES model is shown in Fig. 1. The system model contains two kinds of RE: wind energy and solar energy. The energy conversion relationship in the IES model can be described as follows:

$$\begin{bmatrix} P^t_{l,e} \\ Q^t_{l,c} \\ Q^t_{l,h} \\ V^t_{l,g} \end{bmatrix} = \begin{bmatrix} 1-v_{ec}-v_{eb} & \eta_{chp,e} & 1 & 1 \\ u_2 v_{ec} COP_{ec} & u_2 \eta_{chp,h} COP_{ac} & 0 & 0 \\ u_1 v_{eb} \eta_{eb,h} & u_1 \left(\eta_{chp,h}+\eta_{gb,h}\right) & 0 & 0 \\ 0 & 1-v_{chp}-v_{gb} & 0 & 0 \end{bmatrix} \times \begin{bmatrix} P^t_{buy,e} \\ V^t_{buy,g} \\ P^t_{w,f,e} \\ P^t_{s,f,e} \end{bmatrix} \quad (1)$$

where $P^t_{l,e}$, $Q^t_{l,c}$, $Q^t_{l,h}$ and $V^t_{l,g}$ represent the electric load (EL), cooling load (CL), heating load (HL), and gas load (GL) in the model respectively; $P^t_{buy,e}$ and $V^t_{buy,g}$ represent the electric power purchased from the upper grid and the gas purchased from the upper pipeline; $P^t_{w,f,e}$ and $P^t_{s,f,e}$ represent the electric power generated by WTs and PV units that only consider forecast data; v_{ec}, v_{eb}, v_{chp} and v_{gb} are the distribution coefficients of electric air conditioners (EC), EBs, CHP units and gas boilers (GB) respectively; $\eta_{chp,e}$ and $\eta_{chp,h}$ are the electric power generation coefficient and heating coefficient of CHP units respectively; $\eta_{eb,h}$ and $\eta_{gb,h}$ are the heating coefficient of EBs and GBs respectively; COP_{ec} and COP_{ac} are the refrigeration coefficients of ECs and absorption chillers (AC) respectively; u_1 and u_2 are the binary variable representing the season.

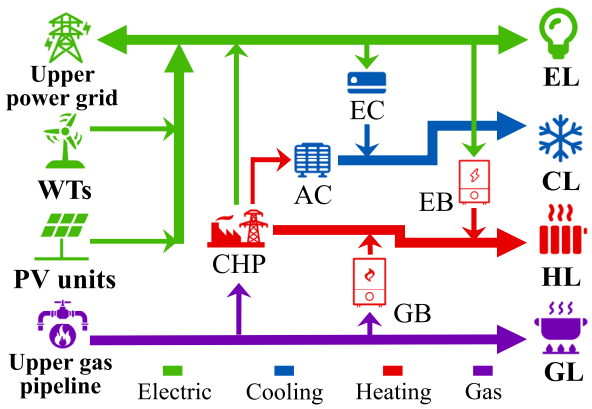

FIGURE 1. The structure diagram of the IES model.

III. SCHEDULING STRATEGY OF IES

The scheduling strategy proposed in this paper is divided into two stages: the day-ahead scheduling stage and the real-time scheduling stage. In the following text, the day-ahead scheduling stage will be referred to as Stage 1, and the real-time scheduling stage (actual operation stage) will be referred to as Stage 2.

The steps of Stage 1 are implemented before the IES actual operation one day in advance. In Stage 1, the day-ahead forecast data of RE is inputted into IES scheduling model. Then through the solution algorithm, the day-ahead optimal scheme can be obtained. The uncertainties of RE are not considered in Stage 1. The day-ahead forecast data of RE is used as the only input data of the scheduling model, so it is assumed that the day-ahead forecast data is the actual output of the RE, and the scheduling model is regarded as a deterministic scheduling model. Therefore, in the day-ahead optimal scheduling scheme, IES can rely on various energy conversion equipment to maximize RE consumption under a specific objective function in a deterministic scenario composed of forecast data.

The day-ahead optimal scheduling scheme is proposed one day before the actual operation of the IES, allowing sufficient preparation time and guiding the pre-scheduling preparations. However, forecast data based on historical data and weather data may deviate from the actual scenario. If no adjustment is made during the actual operation of IES, and the output of each unit in IES is allocated according to the day-ahead optimal scheme, a large amount of energy will be abandoned. Therefore, combining real-time scheduling based on the day-ahead scheme is necessary to achieve a better effect on RE consumption.

The steps of Stage 2 are implemented concurrently with the IES actual operation, which applies real-time scheduling when the day-ahead forecast data deviates from the actual scenario. Therefore, both the output of Stage 1 and the deviation between forecast data and the actual scenario are the inputs of Stage 2. There will be two situations when the deviation occurs: power redundancy or power shortage. The electric power balance is considered foremost under the above two situations. The electric power balance will be regained by adjusting the power generation of CHP units, power purchase from the upper grid, and power consumption of EBs or ECs, based on the day-ahead optimal scheme. As an essential energy conversion equipment in the system, the CHP units act as a heat source in winter, and cooperate with ACs to act as a cold source in summer. While regaining the balance of electric power to change the power generation of CHP units, its heating power output has also changed. Therefore, the heating/cooling power units must also be adjusted at this stage. The scheme in Stage 2 belongs to a scheme of heating/cooling determined by electricity. Fig. 2 illustrates the scheduling principle of Stage 2.

When there is a shortage of electric power in a certain period, the shortage part will be supplemented by increasing

the power generation of CHP units and the power purchase from the upper grid. The power consumption of EBs/ECs will also be reduced to ease the pressure of increasing generation and purchase. When there exists redundant electric power in a certain period, by reducing the generation of CHP units and power purchase from the upper grid, the redundant part can be consumed as much as possible, and the power consumption of EBs/ECs will also be increased to ease the pressure of reducing generation and purchase. The amount of electric power adjustment and deviation must always be balanced to ensure the overall balance of electric power supply and demand. The change in heating power caused by adjusting the electric power must also be balanced to ensure the overall heating balance. In the real-time scheduling process of Stage 2, the balance of electric and heating power must be ensured simultaneously.

Fig. 3 exhibits the process of the two-stage scheduling strategy for IES. The two stages are performed one after the other in sequence. Stage 1 is performed first, which is performed before the IES actual operation one day in advance and based on day-ahead forecast data. Stage 2 is performed after Stage 1 and is synchronized with the IES actual operation, which belongs to real-time scheduling. Stage 2 requires two inputs: the optimal scheme output from Stage 1, the deviation between the actual scenario during IES operation and the forecast data applied in Stage 1.

The optimal scheme output from Stage 1 can only be obtained after Stage 1 is wholly completed. Therefore, Stage 2 must be implemented after Stage 1. By comparing and subtracting between the data obtained in the actual scenario during IES operation and the forecast data applied in Stage 1, another input of Stage 2 called deviation part can be obtained. The deviation part can be straightforward to show how much the output scheme of Stage 2 needs to be adjusted based on the output scheme of Stage 1. Inputting the deviation part into IPSO of Stage 2, the output scheme of Stage 2 can be obtained faster. These two schemes are not independent of each other. The real-time scheduling scheme (output scheme of Stage 2) can be regarded as the adjustment scheme of the day-ahead optimal scheduling scheme (output scheme of Stage 1).

The scheduling model of both stages is solved by IPSO, and its details will be introduced in Section III (A). The objective functions and constraints of the scheduling model of each stage are introduced in Sections III (B) and (C) respectively.

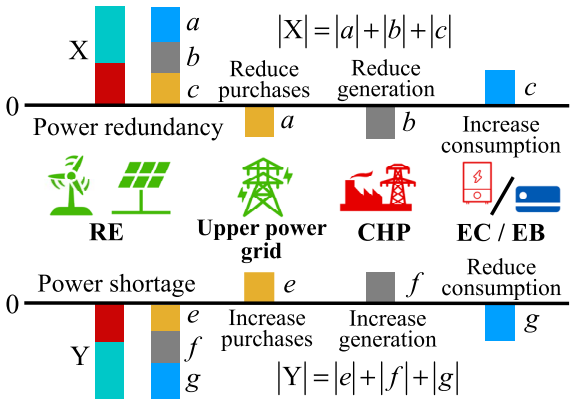

FIGURE 2. The scheduling principle of Stage 2.

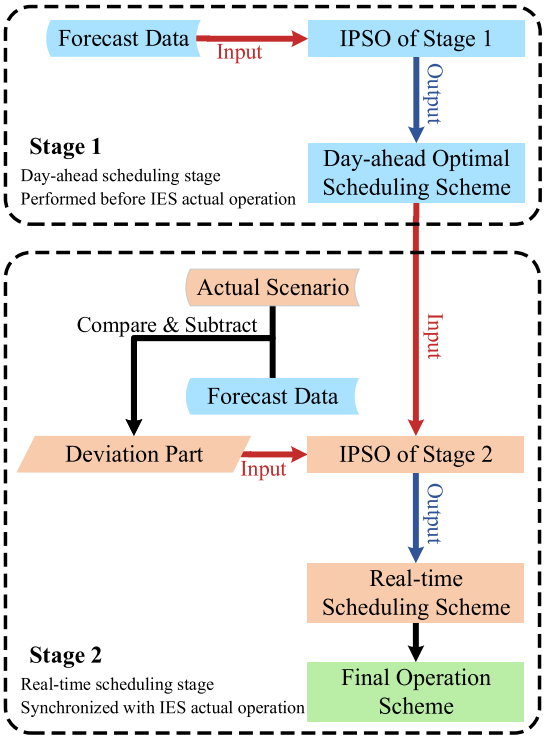

FIGURE 3. The process of two-stage scheduling strategy for IES.

A. IPSO ALGORITHM

PSO is a stochastic optimization algorithm inspired by the social interaction between birds or fish [32], [33], and [34]. PSO is recognized as an intelligent algorithm with concise coding. [35]. In addition, the fast convergence speed of PSO is also very suitable for solving the optimal scheduling problem of IES [36].

The scheduling model describes the nonlinear problem, which contains many constraints and complicated objective functions. The scheduling problem of IES contains many equality constraints relating to the balance of IES, which makes the particles fall into the local optimal solution easily during the iterative process, and thus cannot obtain the proper optimal solution. Therefore, this paper improves PSO by introducing a random nonlinearity change inertia weight strategy and adding the BSPO to propose IPSO, effectively reducing the probability of particles falling into local optimal.

In the PSO, the information carried by each particle is a potential solution. Personal optimal solutions and global optimal solution are obtained through continuous iteration, and the global optimal solution obtained after the iteration will be the optimal solution output by the algorithm. In order to achieve the optimal solution, the iterative formula of particle

velocity and position are described as follows:

$$\begin{cases} v_i^{N_{cur}+1} = \omega v_i^{N_{cur}} + c_1 r_1 \left(p_{best,i}^{N_{cur}} - x_i^{N_{car}} \right) \\ \qquad\qquad + c_2 r_2 \left(g_{best}^{N_{cer}} - x_i^{N_{cur}} \right) \\ x_i^{N_{cur}+1} = x_i^{N_{cur}} + v_i^{N_{cur}} \end{cases} \tag{2}$$

where N_{cur} is current iteration number; $v_i^{N_{cur}}$ and $x_i^{N_{cur}}$ are the velocity and position of particle i at iteration number N_{cur}; $p_{best,i}^{N_{cur}}$ is personal optimal solution of particle i at iteration number N_{cur}; $g_{best}^{N_{cur}}$ is global optimal solution at iteration number N_{cur}; c_1 and c_2 represent acceleration constants; r_1 and r_2 are random numbers distributed between 0 and 1; ω is inertia weight, which is used to balance local exploration and global exploration.

The change strategy of ω in PSO is linear change, which will cause the particles not diversified enough and easily fall into the local optimal. Therefore, the random nonlinearity strategy is introduced to change the inertia weight:

$$\begin{cases} \omega = \omega_{\max} - (\omega_{\max} - \omega_{\min}) \times \left[1 - 2/\left(e^{2N_{cur}/N} + 1\right)\right] \\ rand(N_{cur}) > 0.45 \\ \omega = \omega_{\min} - (\omega_{\max} - \omega_{\min}) \times \left[2N_{cur}/N - (N_{cur}/N)^2\right] \\ rand(N_{cur}) \le 0.45 \end{cases} \tag{3}$$

where $rand(N_{cur})$ is the random probability of the current iteration number; $\omega_{\max}$ and $\omega_{\min}$ are the maximum and minimum values of ω respectively. This strategy makes the adjustment range of ω gradually compressed and shows a nonlinear decreasing trend as a whole. The addition of probability judgment enhances the randomness of ω under the overall decreasing trend prevents ω from falling into a monotonous evolution trend and improves the diversity of particles.

$$b = b_{\max} - \frac{b_{\max} - b_{\min}}{\sum_{n=1}^{cur} N_n} (N - N_{cur}) \tag{4}$$

In order to further prevent the algorithm from falling into the local extremum during the iterative process, the BSPO b has been proposed to adjust personal optimal solutions and the global optimal solution among all particles, so that the particles can escape from the local optimal area, and the search range is expanded. The iterative formula of b can be determined as (4), where N is the maximum iteration number; $b_{\max}$ and $b_{\min}$ are the maximum and minimum values of b respectively. The b decreases nonlinearly as the iteration number increases, which allows particles to perform a large-scale search in the early stage of iteration and a precise search in the later stage of iteration. The addition of b significantly increases the probability of finding the optimal solution. The iterative formula of v_i and x_i after the introduction of the best solution perturbation operator becomes:

$$\begin{cases} v_i^{N_{cur}+1} = \omega v_i^{N_{cur}} + c_1 r_1 \left(b \times p_{best,i}^{N_{cur}} - x_i^{N_{car}} \right) \\ \qquad\qquad + c_2 r_2 \left(b \times g_{best}^{N_{cer}} - x_i^{N_{cur}} \right) \\ x_i^{N_{cur}+1} = x_i^{N_{cur}} + v_i^{N_{cur}} \end{cases} \tag{5}$$

B. DAY-AHEAD OPTIMAL SCHEME

1) OBJECTIVE

Considering the minimization of the economic cost and environmental cost of the IES as the objective of scheduling, the formulation of the objective can be described as follows:

$$C_{obj}^1 = \min \left\{ \alpha_1 (C_{ope} + C_e^1 + C_g) + \alpha_2 C_{env}^1 \right\} \tag{6}$$

$$C_{ope} = C_{chp}^1 + u_1 C_{gb} + u_1 C_{eb} + u_2 C_{ec} + u_2 C_{ac} \tag{7}$$

$$C_e^1 = \sum_{t=1}^{T} c_e^t P_{buy,e}^t \Delta t \tag{8}$$

$$C_g = \sum_{t=1}^{T} c_g V_{buy,g}^t \tag{9}$$

$$C_{env}^1 = c_{CO_2} \eta_{CO_2} \sum_{t=1}^{T} \left(V_{chp,g}^t + u_1 V_{gb,g}^t \right) \tag{10}$$

where C_{ope} is the operating cost of the system; C_e^1 is the cost of electric power purchase in Stage 1; C_g is gas purchase; C_{env}^1 is the cost of environmental protection in Stage 1, which is set to achieve the aim of energy saving and emission reduction; α_1 and α_2 are the weight coefficient of the economic benefits and environmental benefits. Equation (7) shows the operating cost of the system, where C_{chp}^1 is the cost of CHP units in Stage 1; C_{eb}, C_{ec}, C_{gb} and C_{ac} are the cost of EBs, ECs, GBs and ACs respectively. Equation (8) describes the cost of power purchase of the system in Stage 1, where c_e^t is the electricity price of the upper grid for each period; $P_{buy,e}^t$ is the power bought from the upper grid for each period; Δt is the length of the period. Equation (9) describes the cost of gas purchase of the system in Stage 1, where c_g is the price of gas bought from the upper pipeline; $V_{buy,g}^t$ is the amount of gas bought from the upper pipeline for each period. Equation (10) shows the environmental protection cost of the system in Stage 1, where c_{co_2} is the cost of CO_2 emission per unit volume; η_{co_2} is the emission coefficient of CO_2 per unit volume of gas; $V_{CHP,g}^t$ and $V_{GB,g}^t$ are gas consumption of CHP units and GBs for each period respectively.

2) CONSTRAINTS

Equations (11)-(13) describe the output constraints of each unit, where M and K are the collections of all cooling units and heating units respectively; $P_{chp,e}^t$ and $Q_{m,c}^t/Q_{k,h}^t$ represent the output of CHP units and a certain kind of cooling/heating units at t; $P_{chp,e}^{\max}$ and $Q_{m,c}^{\max}/Q_{k,h}^{\max}$ are the maximum output of CHP units and a certain kind of cooling/heating units. Equations (14)-(16) represent the output rising constraints of each unit, where $rP_{chp,e}^{\max}$, $rQ_{m,c}^{\max}$ and $rQ_{k,h}^{\max}$ are the maximum output rising value of CHP units and a certain kind of cooling/heating units. Equations (17) and (18) represent the energy exchange constraints, where $P_{buy,e}^{\max}$ and $V_{buy,g}^{\max}$ are the maximum value of power purchase and gas purchase in a period respectively. The following equations describe system power balance constraints. Equation (19) represents electric power balance. Equation (20) represents cooling or heating

power balance. Equation (21) describes the balance of gas supply and demand. The process of IPSO for the day-ahead optimal scheme is described in Table 1.

$$0 \leqslant P^t_{chp,e} \leqslant P^{\max}_{chp,e} \tag{11}$$
$$0 \leqslant Q^t_{m,c} \leqslant Q^{\max}_{m,c}, \quad m \in M \tag{12}$$
$$0 \leqslant Q^t_{k,h} \leqslant Q^{\max}_{k,h}, \quad k \in K \tag{13}$$
$$P^t_{chp,e} - P^{t-1}_{chp,e} \leqslant rP^{\max}_{chp,e} \tag{14}$$
$$Q^t_{m,c} - Q^{t-1}_{m,c} \leqslant rQ^{\max}_{m,c}, \quad m \in M \tag{15}$$
$$Q^t_{k,h} - Q^{t-1}_{k,h} \leqslant rQ^{\max}_{k,h}, \quad k \in K \tag{16}$$
$$0 \leqslant P^t_{buy,e} \leqslant P^{\max}_{buy,e} \tag{17}$$
$$0 \leqslant V^t_{buy,g} \leqslant V^{\max}_{buy,g} \tag{18}$$
$$P^t_{buy,e} + P^t_{chp,e} + P^t_{w,f,e} + P^t_{s,f,e} = P^t_{l,e} + u_1 P^t_{eb,e} + u_2 P^t_{ec,e} \tag{19}$$
$$Q^t_{m,c} - Q^{t-1}_{m,c} \leqslant rQ^{\max}_{m,c}, \quad m \in M \tag{20}$$
$$Q^t_{k,h} - Q^{t-1}_{k,h} \leqslant rQ^{\max}_{k,h}, \quad k \in K \tag{21}$$

TABLE 1. Process of IPSO in Stage 1.

Algorithm: IPSO for the day-ahead optimal scheme

Input: Forecast data of WTs and PV units ($P^t_{w,f,e}$, $P^t_{s,f,e}$), data of all kinds of loads ($P^t_{l,e}$, $Q^t_{l,c}$ / $Q^t_{l,h}$ and $V^t_{l,g}$).

Output: Power dispatch for each period of the day-ahead optimal scheme ($P^t_{buy,e}$, $P^t_{chp,e}$, $P^t_{w,e}$ and $P^t_{s,e}$; $Q^t_{ec,c}$ and $Q^t_{ac,c}$ / $Q^t_{chp,h}$, $Q^t_{gb,h}$ and $Q^t_{eb,h}$).

Step 1: Set particle swarm size S and particle dimension D
Initialize the particle swarm s_i

Step 2: Set N , c_1 , c_2 , $\omega_{\max}$, $\omega_{\min}$, $b_{\max}$ and $b_{\min}$
Set $N_{cur} = 0$

Step 3: Set $N_{cur} = N_{cur} + 1$

Step 4: If $N_{cur} < N$
Iterating p_i according to (19)-(21)
Obtain the $g^{N_{cer}}_{best}$.
Back to **Step 3**
Else
Go to **Step 5**

Step 5: Take $g^{N_{cer}}_{best}$ as the optimal solution
Output the optimal solution

End

C. REAL-TIME SCHEDULING SCHEME

1) OBJECTIVE

The objective of this stage is still to pursue the minimum cost of the system. This stage is to adjust the day-ahead optimal scheme based on the deviation between forecast data and the actual scenario. Therefore, the parameters in the objective function are composed of the variables of specific costs, which can also improve computational efficiency. The objective function of Stage 2 is as follows:

$$\begin{cases} C^2_{obj} = \min\left\{\Delta C_{chp} + \Delta C_e + \Delta C_{env}\right\} \\ \Delta C_{chp} = C^2_{chp} - C^1_{chp} \\ \Delta C_e = C^2_e - C^1_e \\ \Delta C_{env} = C^2_{env} - C^1_{env} \end{cases} \tag{22}$$

where ΔC_{chp}, ΔC_e and ΔC_{env} are the amount of changes between Stage 1 and Stage 2, in C_{chp}, C_e and C_{env}. The cost of ECs or EBs will also change in the real-time scheduling scheme, but their changes are mainly dependent on the changes of CHP units. Therefore, the cost variation of ECs or EBs is a passive parameter, which is not needed to consider in the objective function.

TABLE 2. Process of IPSO in Stage 2.

Algorithm: IPSO for the real-time scheduling scheme

Input: The output of Stage 1 and the deviation between forecast data and the actual scenario.

Output: Variation of CHP units, purchase from upper grid and ECs/EBs ($\Delta P^t_{chp,e}$, $\Delta P^t_{buy,e}$ and $\Delta P^t_{eb,e}$ / $\Delta P^t_{ec,e}$; $\Delta Q^t_{chp,h}$, $\Delta Q^t_{ec,c}$ / $\Delta Q^t_{eb,h}$).

Step 1: Set particle swarm size S and particle dimension D
Initialize the particle swarm s_i

Step 2: Set N , c_1 , c_2 , $\omega_{\max}$, $\omega_{\min}$, $b_{\max}$ and $b_{\min}$
Set $N_{cur} = 0$

Step 3: Set $N_{cur} = N_{cur} + 1$

Step 4: If $N_{cur} < N$
Iterating s_i according to (19)-(21)
Obtain the $g^{N_{cer}}_{best}$.
Back to **Step 3**
Else
Go to **Step 5**

Step 5: Take $g^{N_{cer}}_{best}$ as the optimal solution
Extract $\Delta P^t_{chp,e}$ and $\Delta P^t_{eb,e}$ / $\Delta P^t_{ec,e}$ from the optimal solution
Calculate $\Delta Q^t_{chp,h}$ / $\Delta Q^t_{ac,c}$ and $\Delta Q^t_{eb,h}$ / $\Delta Q^t_{ec,c}$ based on $\Delta P^t_{chp,e}$
and $\Delta P^t_{eb,e}$ / $\Delta P^t_{ec,e}$

Step 6: Output the results

End

2) CONSTRAINTS

The constraints of the scheduling model in this stage as shown in (23)-(27). They indicate the balance between the electric power adjustment and the deviation, heating power balance during electric power adjustment, and the maximum output rising. Where $\Delta P^t_{chp,e}$, $\Delta P^t_{buy,e}$, $\Delta P^t_{eb,e}$ and $\Delta P^t_{ec,e}$ are the amount of change in $P^t_{chp,e}$, $P^t_{buy,e}$, $P^t_{eb,e}$ and $P^t_{ec,e}$. $P^t_{w,a,e}$ and $P^t_{s,a,e}$ represent the actual output of WTs and PV units. The right side of the equation in (23) expresses the deviation of electric power by making the difference between forecast data and the actual output. Equation (24) describes that the heating

power changes caused by adjusting the electric power distribution should also be balanced. Equations (25)-(27) describe the maximum output rising constraints of CHP units, ECs, and EBs respectively. The process of IPSO for the real-time scheduling scheme is shown in Table 2.

$$\left|\Delta P^t_{buy,e}\right| + \left|\Delta P^t_{chp,e}\right| + u_1\left|\Delta P^t_{eb,e}\right| + u_2\left|\Delta P^t_{ec,e}\right| = \left|(P^t_{w,f,e} + P^t_{s,f,e}) - (P^t_{w,a,e} + P^t_{s,a,e})\right| \quad (23)$$

$$u_1\eta_{chp,h}\frac{\left|\Delta P^t_{chp,e}\right|}{\eta_{chp,e}} + u_2\eta_{chp,h}COP_{ac}\frac{\left|\Delta P^t_{chp,e}\right|}{\eta_{chp,e}} = u_1\eta_{eb,h}\left|\Delta P^t_{eb,e}\right| + u_2COP_{ec}\left|\Delta P^t_{ec,e}\right| \quad (24)$$

$$(P^t_{chp,e} + \Delta P^t_{chp,e}) - (P^{t-1}_{chp,e} + \Delta P^{t-1}_{chp,e}) \leqslant rP^{\max}_{chp,e} \quad (25)$$

$$(Q^t_{ec,c} + \Delta Q^t_{ec,c}) - (Q^{t-1}_{ec,c} + \Delta Q^{t-1}_{ec,c}) \leqslant rQ^{\max}_{ec,c} \quad (26)$$

$$(Q^t_{ec,c} + \Delta Q^t_{ec,c}) - (Q^{t-1}_{ec,c} + \Delta Q^{t-1}_{ec,c}) \leqslant rQ^{\max}_{ec,c} \quad (27)$$

At the algorithm level, the particle swarms initialization, particle iteration and termination conditions of IPSO of stage 1 and IPSO of stage 2 are uniform. The differences between IPSO of stage 1 and IPSO of stage 2 are in terms of inputs, outputs and parameter settings. The differences in inputs and outputs are illustrated in Fig. 3. The difference in parameter settings will be explained in Section IV (A).

IV. CASES STUDY

In this section, the effectiveness of the proposed scheduling strategy is verified. The economic benefits and environmental benefits under different weights are discussed. The performance of IPSO is analyzed depending on the comparison with the other three algorithms.

A. OVERVIEW OF THE CASES

The scheduling strategy proposed in this paper aims to increase RE consumption in IES under the premise of ensuring system benefits. Therefore, the evaluation indicators of this strategy are system benefits, amount of AE, and RECR. Four cases are set in this section. The basic situation of the four cases is as follows:

1) **Case 1:** Without the two-stage strategy proposed in this paper. The day-ahead optimal scheduling scheme is obtained directly from the day-ahead forecast data of RE, and this scheme is implemented during the actual operation. In the process of obtaining the day-ahead optimal scheduling scheme, the weight of the economic benefits α_1 is 0.01, and the weight of the environmental benefits α_2 is 0.99. The uncertainties of RE will cause deviations between the optimal scheduling scheme and the actual scenario. When the electric power is redundant, energy abandonment will occur. When the electric power is short, it will be directly purchased from the upper grid. This is the general scheduling method in the current energy system.
2) **Case 2:** The two-stage scheduling strategy proposed in this paper is applied. Getting the day-ahead optimal scheduling scheme in Stage 1. The real-time scheduling scheme is used to adjust the day-ahead optimal scheduling scheme to overcome the uncertainties of RE in Stage 2. In the process of obtaining the day-ahead optimal scheduling scheme, the weight of the economic benefits α_1 is 0.01, and the weight of the environmental benefits α_2 is 0.99.
3) **Case 3:** Except the weight distribution of economic and environmental benefits is different. Other conditions are the same as in Case 2. In the process of obtaining the day-ahead optimal scheduling scheme, the weight of the economic benefits α_1 is 0.03, and the weight of the environmental benefits α_2 is 0.97.
4) **Case 4:** Except the weight distribution of economic and environmental benefits is different. Other conditions are the same as in Case 2. In the process of obtaining the day-ahead optimal scheduling scheme, the weight of the economic benefits α_1 is 0.003, and the weight of the environmental benefits α_2 is 0.997.

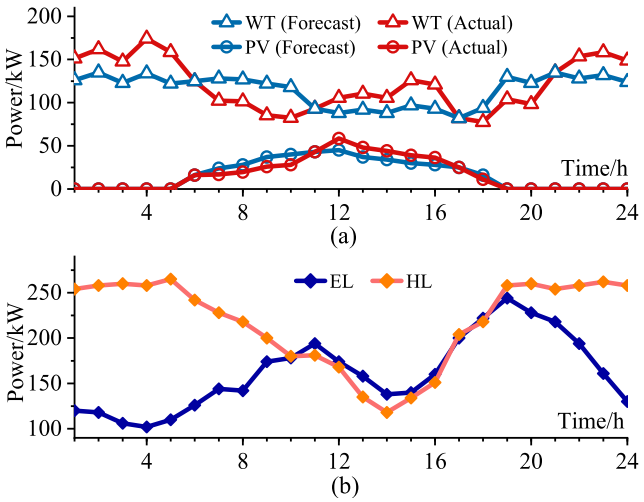

FIGURE 4. Input data of IES model: (a)Forecast data and actual output of WTs and PV units. (b) Electric load and Heating load in the IES.

The weight distribution in Cases 1 and 2 is to keep C_{ope} and C^1_{env} at the same order of magnitude, which considers the economic and environmental benefits comprehensively. The weight distribution in Case 3 attaches more importance to the economic benefits. The weight distribution in Case 4 attaches more importance to the environmental benefits.

The above cases are set according to the control variable method, and Case 2 is the most critical. Cases 1 and 2 use the same weight distribution but different scheduling strategies. Comparing Cases 1 and 2 mainly analyzes the advantages of the two-stage scheduling strategy proposed in this paper. Cases 2, 3 and 4 apply the strategy proposed in this paper but with different weight distributions. Discussing Cases 2, 3 and 4 together is to analyze the results under different weight distributions, which can illustrate the characteristics of the strategy under different weights, and can also reflect the applicability of the strategy under different requirements.

Different regions have different requirements for system scheduling, so discussing IES performance under different requirements can also make the displayed results more valuable.

Although the current technology for forecasting RE output has made significant progress, in order to simulate a more uncertain scenario to verify the effectiveness of the strategy, we still assume that there is a large deviation between forecast data and the actual output. All four cases include two types of RE: WTs and PV units. Fig. 4 (a) shows the curves of forecast data and the actual output of WTs and PV units at each period of a day. We assumed that the actual output of WTs and PV units is based on the forecast data and fluctuates randomly within a range of (-30%, 30%). The simulation scenario we selected is a typical winter day in northern China, with EL and HL included in the IES [18]. Fig. 4 (b) describes the curves of EL and HL in the IES.

In terms of parameters related to the cost of IES, the gas price c_g in cases is 0.5 USD/m^3; c_{CO_2} is set to 10 USD/t and η_{CO_2} is set to 2×10^{-3} t/m^3; the electricity price at each period of the day is not constant, 1:00-7:00 and 21:00-24:00 is 7×10^{-2} USD/kWh; at 8:00 and 13:00-15:00 is 14×10^{-2} USD/kWh; 9:00-12:00 and 16:00-20:00 is 21×10^{-2} USD/kWh. Table 3 shows the parameters of the main energy conversion equipment.

In terms of parameters related to IPSO, in Stage 1 of Cases 2, 3 and 4, S is set to 400, D is set to 7, N is set to 200, c_1 and c_2 are both set to 2.0, $\omega_{\max}$ and $\omega_{\min}$ are set to 0.9 and 0.3 respectively, $b_{\max}$ and $b_{\min}$ are set to 0.8 and 0.3 respectively; in Stage 2 of Cases 2, 3 and 4, S is set to 300, D is set to 6, N is set to 160, and the other parameter settings are uniform with Stage 1. Since Case 1 does not apply the strategy proposed in this paper. The only one stage in the scheduling work of Case 1 is also solved by IPSO, and the parameter settings are consistent with Stage 1 of Cases 2, 3 and 4.

For the algorithm, the solution space and value in Stage 2 are smaller than that of Stage 1, so Stage 2 is more accessible to solve than Stage 1. Therefore, under the premise of ensuring that the optimal result can be output, S and N in Stage 2 can be smaller than that of Stage 1. Moreover, Stage 2 belongs to real-time scheduling, which is performed synchronously with the actual operation of IES. Therefore, IPSO of Stage 2 requires higher computation speed, and smaller S and N are beneficial to improve the computation speed. D represents the amount of information carried by a single particle. Since GB does not participate in the adjustment in Stage 2, the particles in Stage 2 carry one less piece of information than particles in Stage 1. Therefore, D of Stage 2 is one less than that of Stage 1.

In terms of simulation equipment, all simulations are performed on a laptop computer with an i7 3.40 GHz CPU and 16 GB RAM. In terms of software for simulations, the programming of system model, scheduling strategy and solving algorithm is based on MATLAB R2021a and Yalmip. MATLAB R2021a is also used to solve the entire model.

B. ANALYSIS OF STRATEGY EFFECTIVENESS

Before the actual scheduling work, based on the forecast data of RE, the day-ahead optimal scheduling scheme of Cases 1 and 2 is obtained. There is no difference between the day-ahead optimal schemes derived from the two cases.

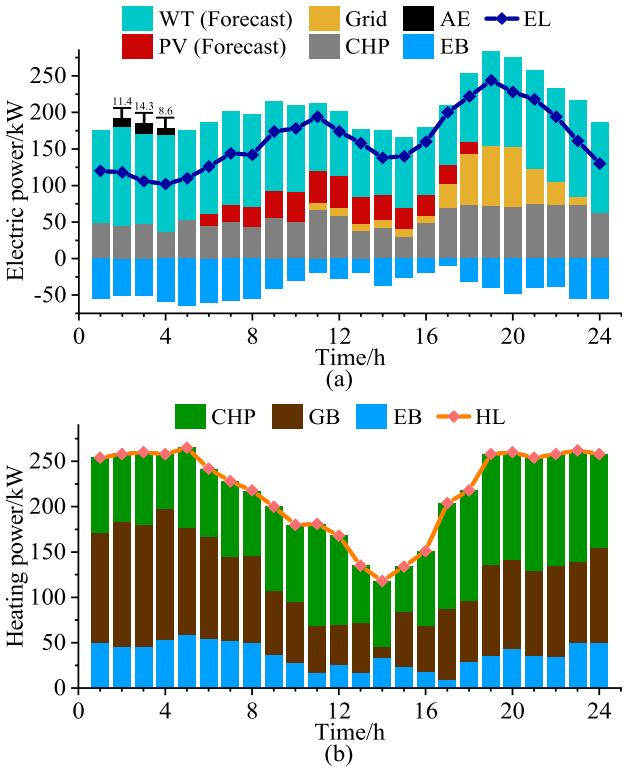

FIGURE 5. Day-ahead optimal scheme of Case 1 and Case 2: (a) Scheduling scheme of electric power. (b) Scheduling scheme of heating power.

The EL peaked at 11:00 and 19:00. According to the climatic characteristics of typical winter days, the HL was high at night and low during the daytime. The scheduling scheme of electric units in each period is shown in Fig. 5 (a). The scheduling scheme of heating units is shown in Fig. 5 (b). Since the day-ahead scheme comprehensively considers the economic and environmental benefits, AE appears but the amount is tiny. There will be a small amount of AE in 2:00-4:00.

Day-ahead scheduling stage of Cases 1 and 2 is identical, but the subsequent process of the two cases is totally different. For Case 1, the day-ahead scheme will be directly applied for the IES actual operation. For Case 2, the day-ahead scheme is just the result of Stage 1, and the day-ahead scheme will undergo real-time scheduling in Stage 2.

The day-ahead scheme obtained before the actual operation can be used as an important basis for the subsequent stage. Due to the forecast data of RE cannot be completely accurate, the situation in the actual operation may be different from the day-ahead scheduling scheme.

Fig. 6 shows the actual operation of Case 1. In Case 1, due to the uncertainties of RE in the actual operation, the

TABLE 3. Parameters of the main energy conversion equipment.

Equipment	Input	Maximum input/h	Conversion efficiency	Output	Maximum output/h
CHP unit	Gas	25 m^3	Electric: 0.3 Heating: 0.5	Electric& Heating	Electric: 75 kW Heating: 125 kW
GB	Gas	19 m^3	0.8	Heating	152 kW
EB	Electric	90 kW	0.9	Heating	81 kW
EC	Electric	30 kW	3.5	Cooling	105 kW
AC	Heating	100 kW	1.2	Cooling	120 kW

TABLE 4. Changes in the power purchase plans of Case 1 and Case 2.

Case \ Period	7:00	8:00	9:00	10:00	18:00	18:00	18:00
1	32.8 kW	33.8 kW	47.7 kW	47.4 kW	21.2 kW	26.0 kW	24.6 kW
2	0 kW	0 kW	0 kW	0 kW	21.2 kW	26.0 kW	24.6 kW

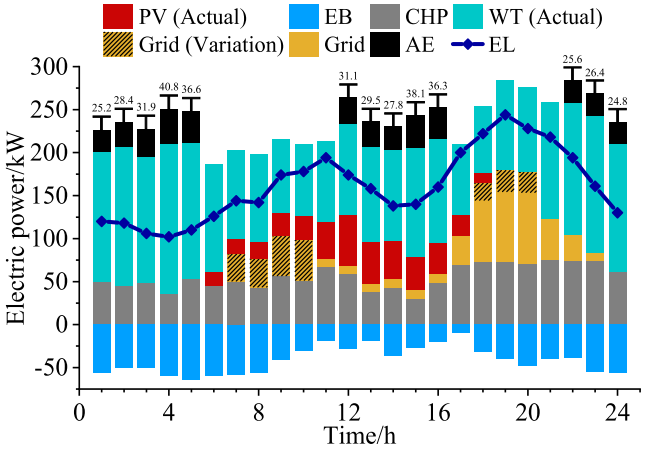

FIGURE 6. Actual operation scheme of electric power in Case 1.

amount of AE is much larger than that in the day-ahead scheme. In Fig.6, AE appears in 1:00-5:00, 12:00-16:00 and 22:00-24:00, and the power purchase plan in the day-ahead scheme is changed in 7:00-10:00 and 18:00-20:00. For Case 1, when forecast data deviates from the actual scenario, the power of each unit in the IES is still distributed according to the day-ahead scheme. Therefore, when the actual output of RE is greater than forecast data, the redundant part is directly abandoned, and when the actual output of RE is less than forecast data, the power purchase is increased to supplement. In Case 1, the energy demands in IES can be guaranteed, but a large amount of RE will be abandoned, and the power purchase plan also has to be changed frequently. The above reasons seriously affect the economic and environmental benefits.

Fig. 7 shows the scheduling scheme in Stage 2 of Case 2. Comparing Fig. 5 (a) and (b) with Fig. 7 (a) and (b), the adjustments based on the day-ahead scheme in Stage 2 can be seen. Except for the four periods where forecast data is identical to the actual scenario (6:00, 11:00, 17:00 and 21:00), the output distributions of the rest periods are adjusted based on the day-ahead scheme. The AE in 2:00 and 3:00 in the day-ahead scheme is absorbed in Stage 2 through the flexible adjustments in real-time scheduling. The AE at 4:00 in the day-ahead scheme is reduced but not fully absorbed in Stage 2. The AE appears at 5:00 in Stage 2, which did not appear in the day-ahead scheme. The reason why the AE at 4:00 is not fully absorbed and the new AE appears at 5:00, is that the deviation between forecast data and the actual scenario is too large, which exceeds the adjustment capability of the CHP units and EBs. With the full use of the capacity of the CHP units and EBs, only a tiny amount of AE occurred at 4:00 and 5:00. If there is no real-time scheduling at 4:00 and 5:00, the AE under such a large deviation will be larger.

Comparing Fig. 6 and Fig. 7 (a), the advantages of the strategy proposed in this paper can be seen. During the periods of electrical power redundancy (1:00-5:00, 12:00-16:00 and 22:00-24:00), the scheme in Case 1 cannot consume the redundant power, and a large amount of AE occurs. The scheme in Case 2 is obtained by the strategy proposed in this paper, which makes AE only appear in two periods (4:00 and 5:00). During the periods of electrical power redundancy (7:00-10:00 and 18:00-20:00), the scheme in Case 1 will increase power purchase directly to fill the shortage. This way requires frequent changes to the power purchase plan, which has a negative impact on the economic benefits of IES. Since the strategy proposed in this paper gives priority to increasing the output of CHP units to fill the shortage, the power purchase plan of Case 2 is only changed in 18:00-20:00. The reason why applying the strategy proposed in this paper still needs to change the plan, is that the shortage exceeds the adjustment range of CHP units.

Fig. 7 (c) exhibits the details of deviations and variations of electric power. The AE in Stage 1 and Stage 2 is different, the AE in Stage 1 represents the energy planned to be abandoned in the day-ahead scheme, and the AE in Stage 2 represents the energy already abandoned during the actual operation. Therefore, when the above two both appear in Fig. 7 (c), we use AE1 to represent the AE in Stage 1 and AE to represent the AE in Stage 2. Fig. 7 (d) exhibits the details of variations in heating power. It can be seen from Fig. 7 (c) and (d) that the electric and heating power can be kept balanced under the real-time scheduling of Stage 2.

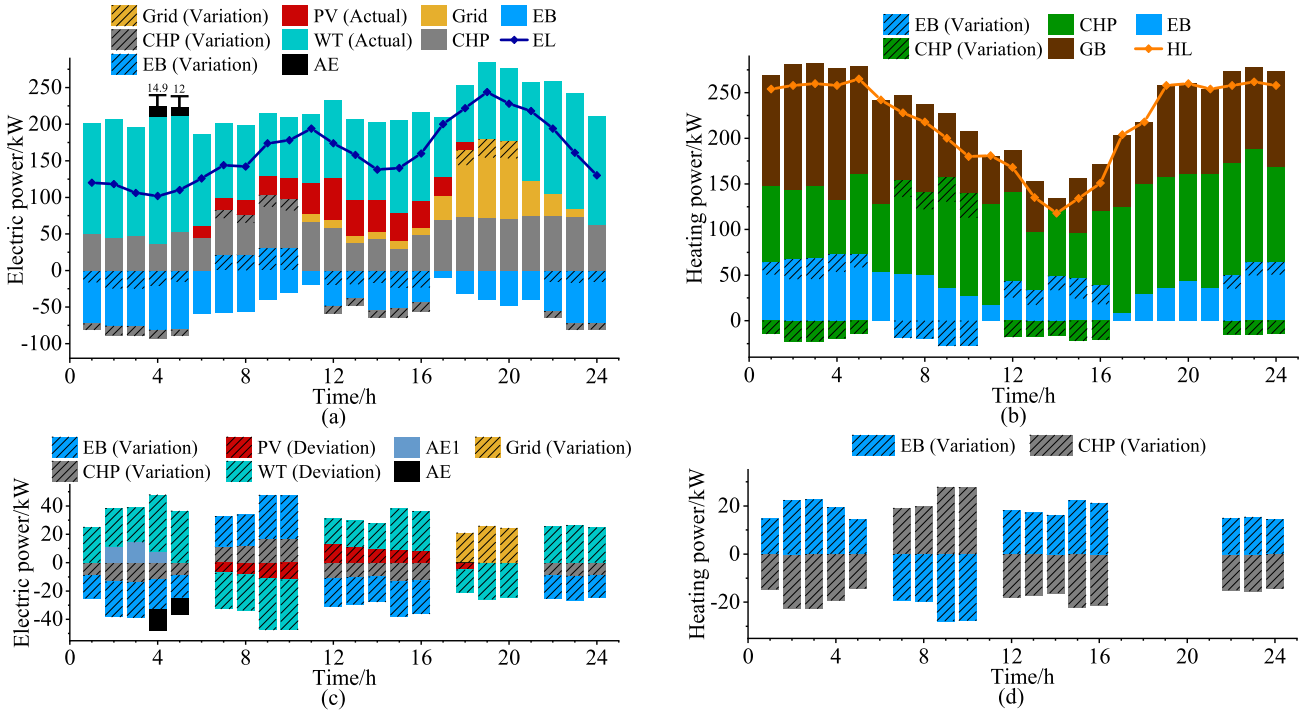

FIGURE 7. Scheduling scheme of Case 2: (a) Scheduling scheme of electric power in Stage 2 (Actual operation scheme). (b) Scheduling scheme of heating power in Stage 2 (Actual operation scheme). (c) Details of deviations and variations of electric power. (d) Details of variation of heating power.

Table 4 compares the changes in the power purchase plans in Case 1 and Case 2. It can be seen from Table 4 that power purchase plan changes in Case 1 are more frequent than that in Case 2. Fig. 10 shows the curve comparisons of RECR in the same stage of different cases. By comparing the RECR curves of Case 1 and Case 2 in Fig. 10, the same conclusion can be drawn as comparing the amount of AE. Case 1 and Case 2 have the same day-ahead scheme obtained in Stage 1, and therefore share one curve in Fig. 10 (a). However, in Stage 2, the RECR of Case 1 in the actual operation deteriorates seriously due to the lack of real-time scheduling. In contrast, the RECR of Case 2 in the actual operation can maintain a high level. Fig. 11 shows the curve comparisons of RECR in the same case at different stages. By observing Fig. 11 (a) and (b), it can be further seen that Case 1 cannot maintain a good RECR in the actual operation without the strategy proposed in this paper. Case 2 applies the strategy proposed in this paper, and the RECR is further improved by real-time scheduling in Stage 2.

Through the above comparisons, it can be seen that applying the strategy proposed in this paper can reduce the number of periods that AE occurs, reduce the total amount of AE, and reduce the number of periods that the power purchase plan is changed. These advantages can significantly improve the RE consumption and benefits of IES.

C. ANALYSIS OF RESULTS UNDER DIFFERENT WEIGHT DISTRIBUTIONS

It can be seen in (6)-(10) that the economic benefit is mainly related to the operating cost of the units and the cost of purchase from the upper system of IES, and the environmental benefit is mainly associated with the carbon emission of the units in IES. Under the same load, if the amount of AE is small and the RECR is high, then the output of CHP and GB in the system will be relatively reduced, so that the carbon emissions will be reduced, and the environmental benefits will be better. On the contrary, the environmental benefits will be worse. Therefore, the environmental benefits are closely related to the amount of AE and RECR.

Based on different weight distributions of the economic and environmental benefits, Case 3 attaches more importance to the economic benefits and Case 4 attaches more importance to the environmental benefits. The scheme in Stage 1 of Cases 3 and 4 is shown in Fig. 8 (a) and Fig. 9 (a). Comparing Fig. 5 (a), Fig. 8 (a) and Fig. 9 (a), it can be seen that Case 3 has the most AE in the day-ahead scheme, no AE in the day-ahead scheme of Case 4, and AE in the day-ahead scheme of Case 2 was between Case 3 and Case 4. In the 1:00-8:00 of the scheme, the EL is low, and the HL and WTs output are high. The capacity of EBs in the IES model is sufficient to satisfy HL alone, and increasing the output of EBs can not only fit the higher HL, but also consume the output of WTs. However, the extensive cost of EBs will increase the operating cost of the IES, which affects the economic benefits of IES. In Case 3, which focuses more on the economic benefits, the day-ahead scheme output by the scheduling strategy does not sacrifice the economic benefits in order to consume more RE. On the contrary, Case 4 focuses more on the environmental benefits, the day-ahead scheme uses the capacity of EB to completely absorb RE, which can significantly improve

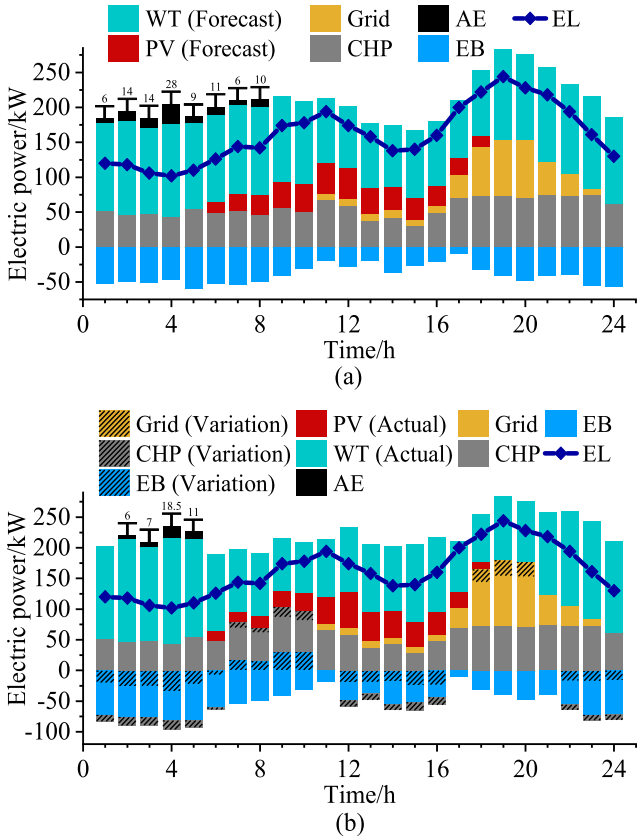

FIGURE 8. Scheduling scheme of electric power in Case 3: (a) Scheduling scheme in Stage 1 (Day-ahead scheduling scheme). (b) Scheduling scheme in Stage 2 (Actual operation scheme).

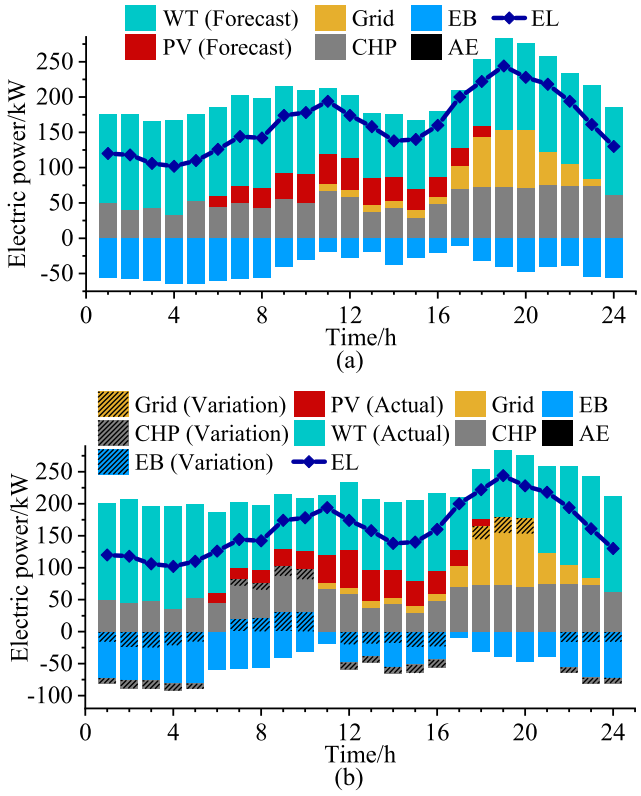

FIGURE 9. Scheduling scheme of electric power in Case 4: (a) Scheduling scheme in Stage 1 (Day-ahead scheduling scheme). (b) Scheduling scheme in Stage 2 (Actual operation scheme).

the environmental benefits of IES. Comparing Fig. 7 (a), Fig. 8 (b) and Fig. 9 (b), it can be seen that the conclusion of comparing the three cases in Stage 1 still applies in Stage 2. Case 3 still has the most AE in Stage 2, but under the effect of real-time scheduling, the period with AE has dropped from 8 to 4. Case 4 still completely consumes RE under the real-time scheduling of Stage 2. The amount of AE of Case 2 in Stage 2 is still between Case 3 and Case 4.

A conclusion can be obtained by comparing the RECR of the three cases in Fig. 10, which is the same as the conclusion obtained by comparing the AE amounts. The RECR of Case 3, which attaches more importance to the economic benefits, is the lowest among the three in both stages. While the RECR of Case 4, which attaches more importance to the environmental benefits, remains at the highest level in both stages. By observing Fig. 11, it can be seen that, except that RECR of Case 4 is kept at the highest level in both stages, RECR of the other two cases under different weight distributions both have improvement through the real-time scheduling. The difference in the magnitude of the improvement is due to the different weight distributions.

The cost of each case is shown in Table 5. The rank of the economic benefits is Cases 3 better than Case 2 better than Case 4. The rank of the environmental benefits is Cases 4 better than Case 2 better than Case 3. Whatever economic or environmental benefits, Cases 2, 3, and 4 with the strategy proposed in this paper are better than Case 1.

Different weight distributions can reflect different scheduling requirements. Therefore, through the above analyses, the operation characteristics of the strategy proposed in this paper under different scheduling requirements can be seen, and it can be derived that the strategy proposed in this paper is suitable for various scheduling requirements. The scheme obtained in Case 3 is suitable for some areas where environmental problems are not severe and require high economic benefits. The scheme obtained in Case 4 is suitable for areas with severe environmental pollution and regards environmental protection as the primary goal.

TABLE 5. Cost of each case.

Cost/$ \ Case	1	2	3	4
Operation	5165	5025	4930	5238
Environment	58	46	56	35

D. ANALYSIS OF IPSO PERFORMANCE

In order to reflect that IPSO has more excellent performance for solving the scheduling model, four intelligent algorithms have been selected to observe their performance in solving IES scheduling model, and compare their computation cost and time under the same running situation. We selected IPSO,

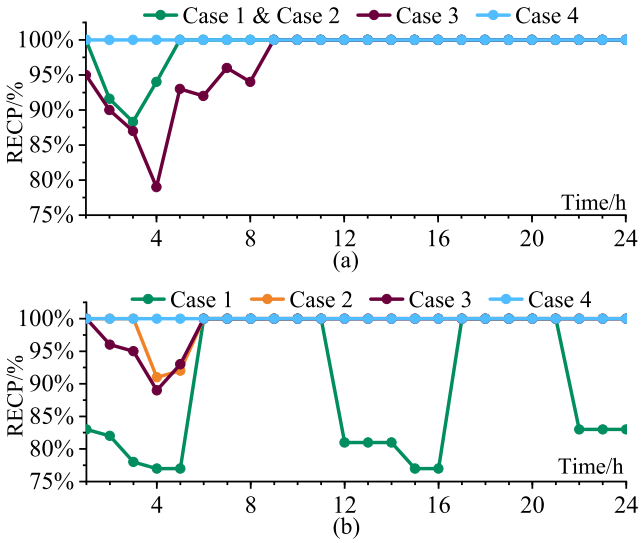

FIGURE 10. Curve comparisons of RECR in the same stage of different cases: (a) Curve comparison of RECR in Stage 1 (Day-ahead scheduling). (b) Curve comparison of RECR in Stage 2 (Actual operation).

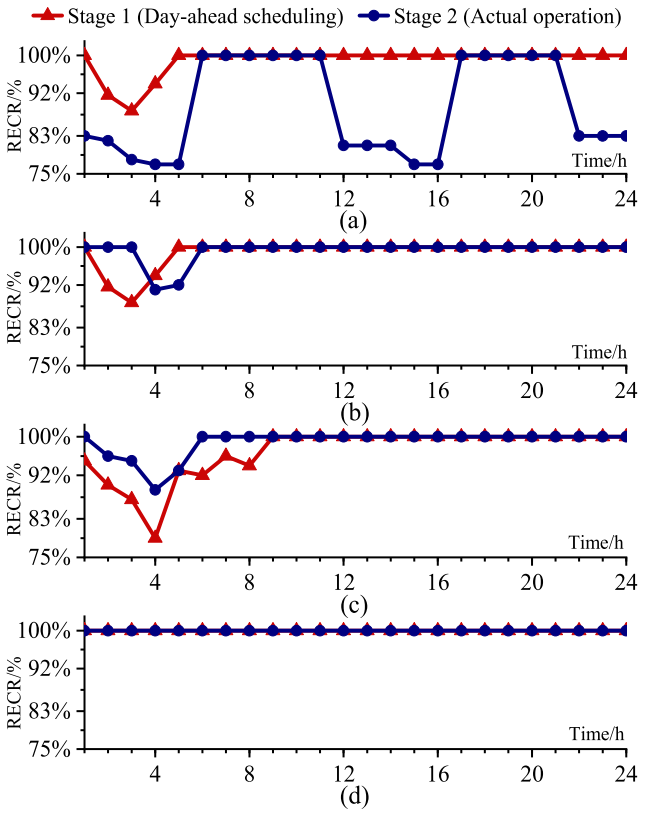

FIGURE 11. Curve comparisons of RECR in the same case at different stages: (a) Curve comparison of RECR in Case 1. (b) Curve comparison of RECR in Case 2. (c) Curve comparison of RECR in Case 3. (d) Curve comparison of RECR in Case 4.

PSO, GA (genetic algorithm) and GWO (gray wolf optimization), which are commonly applied to solve scheduling models.

The indicators for evaluating the performance of different algorithms when solving the scheduling model include convergence speed and calculation accuracy. The comparison of the above indicators is illustrated in Fig. 12. The purpose of comparing computation cost and time under the same running situation is to demonstrate the operating characteristics and requirements of each algorithm, and these comparison results can provide a reference for the staff who choose this strategy. The data of computation cost and time are summarized in Table 6.

The process of using the algorithm to solve the scheduling model in this work is: finding the optimal scheme for each period according to the time sequence, and the optimal scheme for each period is combined to form the whole optimal scheme, so that the algorithm optimization is implemented on every period. In order to be fair in the comparison, the first period of Stage 1 in Case 2 is selected as the common solution object of the four algorithms. The termination conditions of the iteration are uniformly set as: reaching the maximum iteration number (N), and N is uniformly set to 400. In fact, IPSO does not need to set such a large N due to the fast convergence speed. But in order to be consistent with other algorithms in the comparison, the N of IPSO is also set to 400.

Compared with PSO, the convergence speed of IPSO and PSO is close. The convergence speed of PSO is very fast, but it falls into the local optimal and fails to obtain the global optimal solution, while the IPSO solution result is the global optimal solution. The solution accuracy of GWO is better than that of PSO, but the solution accuracy and convergence speed are inferior to IPSO. Based on the crossover and mutation of its process, the solution result of GA is closest to the global optimal solution, but it has not reached the accuracy of IPSO, and the convergence speed of GA is too slow, which will affect the process of scheduling work. From the above analysis, it can be seen that after the improvement of this paper, the IPSO has an excellent solution accuracy for IES scheduling model based on the reduced probability of falling into local optimal. Moreover, the improvement of IPSO did not affect its convergence speed, which is also particularly important in scheduling work.

The data in Table 6 shows that the computation time of IPSO is shorter than that of GA and GWO. However, due to the addition of random nonlinearity change inertia weight strategy and BSPO, the computation time of IPSO is slightly longer than that of PSO. Since the solution object of four algorithms is only one period, their calculation time in this comparison is very short, and the difference is not obvious. When solving the optimal result of multiple periods, the gap in calculation time between each algorithm will be enlarged.

Since the utilization of CPU and RAM is constantly fluctuating during the running process, the utilization of CPU and RAM in Table 6 are the average values during the running process. The utilization of CPU and RAM of IPSO is lower than that of GA and GWO, which means that the computation cost of IPSO is lower than that of GA and GWO, which can reflect that IPSO does not have high requirements on the configuration of computing equipment. However, the

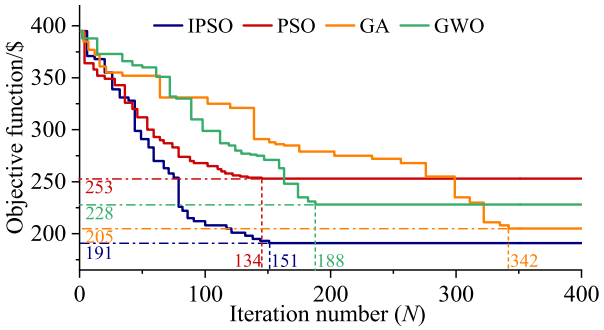

FIGURE 12. Performance of solving IES scheduling model of IPSO, PSO, GA and GWO.

TABLE 6. Computation cost & time of IPSO, PSO, GA and GWO.

Algorithm	IPSO	PSO	GA	GWO
Time/s	23	21	28	26
CPU utilization/%	67	64	71	73
RAM utilization/%	31	27	39	37

computation cost of IPSO is slightly higher than that of PSO, which is also due to the addition of random nonlinearity change inertia weight strategy and BSPO. The computation cost of IPSO is not much higher than that of PSO, which is entirely acceptable. Therefore, the computation cost required by IPSO is fully applicable to most computing equipment.

V. CONCLUSION

As one of the main methods to solve the problems of IES, an intelligent scheduling strategy can significantly improve energy efficiency and RE consumption. In this work, focusing on the problem of deviation between the day-ahead scheme and the actual scenario caused by the uncertainties of RE, a two-stage scheduling strategy for IES is proposed.

Firstly, the model of IES contains many energy conversion equipment is established, which can distribute energy reasonably through flexible energy conversion. This model is the basis for implementing the strategy. Secondly, the scheduling strategy is proposed, which consists of two stages: day-ahead scheduling and real-time scheduling. Day-ahead scheduling stage can output the day-ahead optimal scheduling scheme one day in advance, which can provide early guidance for the preparation of IES operation. The real-time scheduling stage is synchronized with the actual operation of IES and outputs the real-time scheduling scheme, which is the adjustment based on the day-ahead scheme. Thirdly, by introducing random nonlinearity change inertia weight strategy and BSPO, IPSO is proposed as the solution algorithm of the scheduling model.

Finally, the results and analyses in Cases Study demonstrate the conclusions as follows:

1) Under the premise of ensuring system benefits, the strategy proposed in this paper can effectively improve RE consumption and reduce the amount of AE.
2) The strategy performs different operating characteristics under different weight distributions, and is applicable under different scheduling requirements.
3) IPSO has better solution accuracy and faster solution speed when compared with the other three algorithms, which makes it has better performance for solving IES scheduling model.

In future work, we plan to consider the possible failures in IES operation process, analyze the impact of the potential failures, and propose a strategy to obtain an optimal scheme after failures.

REFERENCES

[1] Z. Xu, G. Han, L. Liu, M. Martinez-Garcia, and Z. Wang, "Multi-energy scheduling of an industrial integrated energy system by reinforcement learning-based differential evolution," *IEEE Trans. Green Commun. Netw.*, vol. 5, no. 3, pp. 1077–1090, Sep. 2021.
[2] J. Tian, R. Xu, Y. Wang, and Z. Chen, "Capacity attenuation mechanism modeling and health assessment of lithium-ion batteries," *Energy*, vol. 221, Apr. 2021, Art. no. 119682.
[3] Y. Ding, Q. Xu, Y. Xia, J. Zhao, X. Yuan, and J. Yin, "Optimal dispatching strategy for user-side integrated energy system considering multiservice of energy storage," *Int. J. Electr. Power Energy Syst.*, vol. 129, Jul. 2021, Art. no. 106810.
[4] C. Yang and Y. Zhu, "Two-time scaled identification for multi-energy systems," *Control Eng. Pract.*, vol. 113, Aug. 2021, Art. no. 104845.
[5] S. Zhang, W. Gu, S. Yao, S. Lu, S. Zhou, and Z. Wu, "Partitional decoupling method for fast calculation of energy flow in a large-scale heat and electricity integrated energy system," *IEEE Trans. Sustain. Energy*, vol. 12, no. 1, pp. 501–513, Jan. 2021.
[6] V.-H. Bui, A. Hussain, Y.-H. Im, and H.-M. Kim, "An internal trading strategy for optimal energy management of combined cooling, heat and power in building microgrids," *Appl. Energy*, vol. 239, pp. 536–548, Apr. 2019.
[7] C. Lingmin, W. Jiekang, W. Fan, T. Huiling, L. Changjie, and X. Yan, "Energy flow optimization method for multi-energy system oriented to combined cooling, heating and power," *Energy*, vol. 211, Nov. 2020, Art. no. 118536.
[8] J. Chang, Z. Li, Y. Huang, X. Yu, R. Jiang, R. Huang, and X. Yu, "Multi-objective optimization of a novel combined cooling, dehumidification and power system using improved M-PSO algorithm," *Energy*, vol. 239, Jan. 2022, Art. no. 122487.
[9] E. S. Parizy, S. Choi, and H. R. Bahrami, "Grid-specific co-optimization of incentive for generation planning in power systems with renewable energy sources," *IEEE Trans. Sustain. Energy*, vol. 11, no. 2, pp. 947–957, Apr. 2020.
[10] Y. Liu, S. Xie, Q. Yang, and Y. Zhang, "Joint computation offloading and demand response management in mobile edge network with renewable energy sources," *IEEE Trans. Veh. Technol.*, vol. 69, no. 12, pp. 15720–15730, Dec. 2020.
[11] W. Jiang, K. Yang, J. Yang, R. Mao, N. Xue, and Z. Zhuo, "A multiagent-based hierarchical energy management strategy for maximization of renewable energy consumption in interconnected multi-microgrids," *IEEE Access*, vol. 7, pp. 169931–169945, 2019.
[12] Z. Guo, W. Wei, L. Chen, Z. Y. Dong, and S. Mei, "Impact of energy storage on renewable energy utilization: A geometric description," *IEEE Trans. Sustain. Energy*, vol. 12, no. 2, pp. 874–885, Apr. 2021.
[13] J. Li, Y. Fu, C. Li, J. Li, Z. Xing, and T. Ma, "Improving wind power integration by regenerative electric boiler and battery energy storage device," *Int. J. Electr. Power Energy Syst.*, vol. 131, Oct. 2021, Art. no. 107039.
[14] Y. Ma, Y. Yu, and Z. Mi, "Accommodation of curtailed wind power by electric boilers equipped in different locations of heat-supply network for power system with CHPs," *J. Modern Power Syst. Clean Energy*, vol. 9, no. 4, pp. 930–939, 2021.
[15] H. Mehrjerdi, R. Hemmati, M. Shafie-khah, and J. P. S. Catalao, "Zero energy building by multicarrier energy systems including hydro, wind, solar, and hydrogen," *IEEE Trans. Ind. Informat.*, vol. 17, no. 8, pp. 5474–5484, Aug. 2021.
[16] Z. Zeng, T. Ding, Y. Xu, Y. Yang, and Z. Dong, "Reliability evaluation for integrated power-gas systems with power-to-gas and gas storages," *IEEE Trans. Power Syst.*, vol. 35, no. 1, pp. 571–583, Jan. 2020.

[17] X. Liu, S. Xie, C. Geng, and H. Cao, "Operation strategy for community integrated energy systems considering wind and solar power consumption," in *Proc. 40th Chin. Control Conf. (CCC)*, Shanghai, China, Jul. 2021, pp. 5764–5769.

[18] S. Lu, W. Gu, S. Zhou, S. Yao, and G. Pan, "Adaptive robust dispatch of integrated energy system considering uncertainties of electricity and outdoor temperature," *IEEE Trans. Ind. Informat.*, vol. 16, no. 7, pp. 4691–4702, Jul. 2020.

[19] B. Tan, H. Chen, X. Zheng, and J. Huang, "Two-stage robust optimization dispatch for multiple microgrids with electric vehicle loads based on a novel data-driven uncertainty set," *Int. J. Electr. Power Energy Syst.*, vol. 134, Jan. 2022, Art. no. 107359.

[20] H.-T. Yang, C.-M. Huang, Y.-C. Huang, and Y.-S. Pai, "A weather-based hybrid method for 1-day ahead hourly forecasting of PV power output," *IEEE Trans. Sustain. Energy*, vol. 5, no. 3, pp. 917–926, Jul. 2014.

[21] M. J. Sanjari, H. B. Gooi, and N.-K. C. Nair, "Power generation forecast of hybrid PV-wind system," *IEEE Trans. Sustain. Energy*, vol. 11, no. 2, pp. 703–712, Apr. 2020.

[22] Y. Sun, B. Zhang, L. Ge, D. Sidorov, J. Wang, and Z. Xu, "Day-ahead optimization schedule for gas-electric integrated energy system based on second-order cone programming," *CSEE J. Power Energy Syst.*, vol. 6, no. 1, pp. 142–151, Mar. 2020.

[23] Y. Yin, T. Liu, L. Wu, C. He, and Y. Liu, "Day-ahead risk-constrained stochastic scheduling of multi-energy system," *J. Modern Power Syst. Clean Energy*, vol. 9, no. 4, pp. 720–733, 2021.

[24] X. Liu, S. Xie, C. Geng, J. Yin, G. Xiao, and H. Cao, "Optimal evolutionary dispatch for integrated community energy systems considering uncertainties of renewable energy sources and internal loads," *Energies*, vol. 14, no. 12, p. 3644, Jun. 2021.

[25] J. Zhang, D. Qin, Y. Ye, Y. He, X. Fu, J. Yang, G. Shi, and H. Zhang, "Multi-time scale economic scheduling method based on day-ahead robust optimization and intraday MPC rolling optimization for microgrid," *IEEE Access*, vol. 9, pp. 140315–140324, 2021.

[26] Y. Allahvirdizadeh, S. Galvani, and H. Shayanfar, "Data clustering based probabilistic optimal scheduling of an energy hub considering risk-averse," *Int. J. Electr. Power Energy Syst.*, vol. 128, Jun. 2021, Art. no. 106774.

[27] M. Jadidbonab, B. Mohammadi-Ivatloo, M. Marzband, and P. Siano, "Short-term self-scheduling of virtual energy hub plant within thermal energy market," *IEEE Trans. Ind. Electron.*, vol. 68, no. 4, pp. 3124–3136, Apr. 2021.

[28] M. Alipour, K. Zare, and M. Abapour, "MINLP probabilistic scheduling model for demand response programs integrated energy hubs," *IEEE Trans. Ind. Informat.*, vol. 14, no. 1, pp. 79–88, Jan. 2018.

[29] E. Mokaramian, H. Shayeghi, F. Sedaghati, A. Safari, and H. H. Alhelou, "An optimal energy hub management integrated EVs and RES based on three-stage model considering various uncertainties," *IEEE Access*, vol. 10, pp. 17349–17365, 2022.

[30] M. Kermani, E. Shirdare, A. Najafi, B. Adelmanesh, D. L. Carni, and L. Martirano, "Optimal self-scheduling of a real energy hub considering local DG units and demand response under uncertainties," *IEEE Trans. Ind. Appl.*, vol. 57, no. 4, pp. 3396–3405, Jul. 2021.

[31] B. Farshidian and A. R. Ghahnavieh, "A comprehensive framework for optimal planning of competing energy hubs based on the game theory," *Sustain. Energy, Grids Netw.*, vol. 27, Sep. 2021, Art. no. 100513.

[32] A. Ahilan, G. Manogaran, C. Raja, S. Kadry, S. N. Kumar, C. A. Kumar, T. Jarin, S. Krishnamoorthy, P. M. Kumar, G. C. Babu, N. S. Murugan, and Parthasarathy, "Segmentation by fractional order Darwinian particle swarm optimization based multilevel thresholding and improved lossless prediction based compression algorithm for medical images," *IEEE Access*, vol. 7, pp. 89570–89580, 2019.

[33] L. Zhang and L. Zhao, "High-quality face image generation using particle swarm optimization-based generative adversarial networks," *Future Gener. Comput. Syst.*, vol. 122, pp. 98–104, Sep. 2021.

[34] T. Dutta, S. Dey, S. Bhattacharyya, and S. Mukhopadhyay, "Quantum fractional order Darwinian particle swarm optimization for hyperspectral multi-level image thresholding," *Appl. Soft Comput.*, vol. 113, Dec. 2021, Art. no. 107976.

[35] T. Dutta, S. Dey, S. Bhattacharyya, and S. Mukhopadhyay, "Quantum fractional order Darwinian particle swarm optimization for hyperspectral multi-level image thresholding," *Appl. Soft Comput.*, vol. 113, Dec. 2021, Art. no. 107976.

[36] R. Wang, K. Hao, L. Chen, T. Wang, and C. Jiang, "A novel hybrid particle swarm optimization using adaptive strategy," *Inf. Sci.*, vol. 579, pp. 231–250, Nov. 2021.

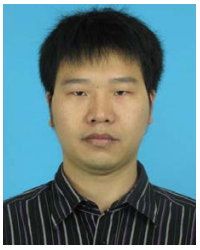

XINGHUA LIU (Senior Member, IEEE) received the B.Sc. degree from Jilin University, Changchun, China, in 2009, and the Ph.D. degree in automation from the University of Science and Technology of China, Hefei, China, in 2014.

From 2014 to 2015, he was invited as a Visiting Fellow with RMIT University, Melbourne, VIC, Australia. From 2015 to 2018, he was a Research Fellow with the School of Electrical and Electronic Engineering, Nanyang Technological University, Singapore. He has been a Professor with the Xi'an University of Technology, Xi'an, China, since 2018. His current research interests include integrated energy systems, intelligent systems, cyber-physical systems, robotic systems, state estimation and control, and autonomous vehicles.

SHENGHAN XIE (Student Member, IEEE) received the B.S. degree in electrical engineering from the Xi'an University of Architecture and Technology, Xi'an, in July 2020. He is currently pursuing the M.S. degree with the Xi'an University of Technology, Xi'an, China.

His research interests include renewable energy consumption and failure state operation of integrated energy systems.

JIAQIANG TIAN received the B.S. degree in automation from Xi'an Technological University, Xi'an, China, in 2016, and the Ph.D. degree in control science and engineering from the University of Science and Technology of China, Hefei, China, in 2021.

He has been joining the Xi'an University of Technology as a Lecturer, since July 2021. His research interests include energy storage modeling, fault diagnosis and energy management, and optimal scheduling of integrated energy systems.

PENG WANG (Fellow, IEEE) received the B.Sc. degree from Xi'an Jiaotong University, Xi'an, China, in 1978, the M.Sc. degree from the Taiyuan University of Technology, Taiyuan, China, in 1987, and the M.Sc. and Ph.D. degrees from the University of Saskatchewan, Saskatoon, SK, Canada, in 1995 and 1998, respectively, all in electrical engineering.

He is currently a Professor at Nanyang Technological University, Singapore. His research interests include power system planning and operation, renewable energy planning, solar/electricity conversion systems, and power system reliability analysis. He served as an Associate Editor of the IEEE TRANSACTION ON SMART GRID and a Guest Editor of *Journal of Modern Power Systems and Clean Energy* for special issues on Smart Grids. He also served as an Associate Editor of IEEE TRANSACTION ON POWER DELIVERY and the Guest Editor-in-Chief of *CSEE Journal of Power and Energy Systems* for special issues on Hybrid AC/DC Grids for Future Power Systems.